Analysis of force and deformation characteristics in geosynthetic-reinforced structures

Shu-Gang Ai, Hong-Xin Chen, & Shi-Jin Feng

Tongji University, China

ABSTRACT: Soil arching and membrane effect often occur simultaneously in geosynthetic-reinforced structures subjected to localized sinkholes. An analytical model is proposed to estimate the force and deformation characteristics of soil and geosynthetic. This model couples the arching effect occurred in overlying soil and the membrane effect of deflected geosynthetic. During subsidence, the upper interface friction between soil and geosynthetic is considered and the deformation of soil agrees with one-dimensional compression model. The forces and deformations of soil and geosynthetic after subsidence can be determined by considering the soil-geosynthetic interaction in subsided and anchorage areas. The maximum geosynthetic strain and the maximum surface settlement, served as key design points, can be obtained. The effects of supporting soil on soil arching and membrane effect are analyzed based on the proposed model. The results show that ignoring the supporting soil in subsided area leads to obvious undervaluation of arching effect and membrane effect, and the force-deformation relationship of supporting soil is of importance for rational design of geosynthetic-reinforced structures.

Keywods: Geosynthetic; Soil arching; Membrane effect; Force; Deformation

1 INTRODUCTION

Geosynthetic-reinforced structures are extensively used in geotechnical engineering. Soil arching and membrane effect often occur simultaneously in such a~~n~~ structure where subsoil may have differential settlement, sinkholes due to karstic collapse, soil dissolution, fissures and cracks, and localized subsidence (Giroud et al. 1990). Geosynthetic interacts with overlying soil even supporting soil during subsidence. Soil arching reflects load transmission from subsided zone to surrounding less-deformed zone, and membrane effect represents load-deformation coordination of deflected geosynthetic (van Eekelen et al. 2013, Lu and Miao 2015, Feng et al. 2017a, b). The two codetermine the maximum tensile strain of geosynthetic and maximum surface settlement, served as key design points of geosynthetic reinforcement (Espinoza 1994, Briançon and Villard 2008, Villard et al. 2016). Therefore, it is essential to have a better understanding of mechanism of soil-geosynthetic interaction for rational design of geosynthetic-reinforced structures.

To evaluate the soil arching for geosynthetic-reinforced structures, Terzaghi (1943) originally imagined an infinitely high soil arch in which lateral load transfer is achieved through shear stresses along vertical planes located at the edges of the subsidence area. Then, the results of trapdoor experiments indicate that the scope of soil arching changes with different subsidence displacements (Evans 1984, Dewoolkar et al. 2007). Based on this, Lu and Miao (2015) proposed a simplified method by evaluating the soil-geosynthetic interaction based on the arching effect considering non-fully mobilized shear stress with the assumption of minor principal stress trajectory. However, the authors adopted a constant lateral earth pressure coefficient, independent of depth, which means all the soil elements in the scope of soil arching have the same deflection, which obviously flies in the face of the real scenario provided by Rui et al. (2016a, b). Lately, Feng et al. (2017a) made contribution to solve such a problem like this by considering the deformation of subsided soil.

For membrane effect, Espinoza (1994) deduced non-uniform strain of deflected geosynthetic with irregular shape based on its force equilibrium conditions. Then, Gourc and Villard (2000) obtained the maximum deflection and maximum tensile force for serviceability design of geosynthetic-reinforced structures over cavity. Based on this, Feng et al. (2017a) analyzed the force and deformation characteristics by coupling arching effect and membrane effect. But at this point, the slippage between soil and geosynthetic has not been taken into account, which changes the external load on deflected geosynthetic and then affects the estimation of arching effect and membrane effect. Therefore, it is necessary to improve the evaluation model based on the coupled model proposed by Feng et al. (2017a).

This paper proposes an analytical model to couple soil arching with membrane effect in geosynthetic-reinforced structures under localized sinkholes. Arching effect can be determined based on the stress and deformation of subsided soil over geosynthetic. Membrane effect is evaluated with consideration of the upper interface friction between soil and geosynthetic. The two are coupled by means of the force equilibrium and deformation coordination between soil and geosynthetic. The force and deformation characteristics are analyzed using the proposed model. The analysis can be useful for rational design of geosynthetic-reinforced structures subjected to localized sinkholes.

2 ANALYTICAL MODEL

A geosynthetic-reinforced structure consists of overlying soil, geosynthetic and supporting soil (Figure 1). During a subsiding process, all three deform simultaneously in the vertical direction. Arching effect occurs in the overlying soil. The deformed overlying soil deflects the geosynthetic, and then the supporting soil. The deflected geosynthetic served as a reinforcement, instead, stops the overlying soil sinking (i.e., membrane effect). Thus, estimation of geosynthetic reinforcement can be achieved by coupling the arching effect of overlying soil and the membrane effect of deflected geosynthetic. A coupled analytical model is proposed in the later part.

2.1 *Arching effect from overlying soil*

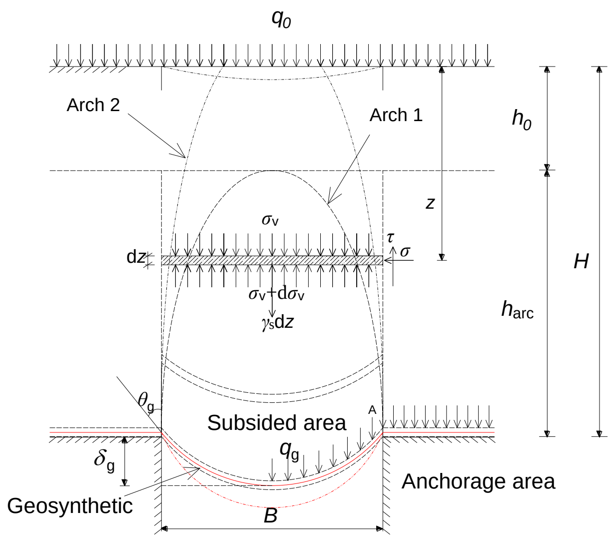

Figure 1. Deformations of the overlying soil and geosynthetic after subsidence.

In this study, the deformed soil above the geosynthetic is assumed to slide along vertical planes located at the edges of subsidence area, which has been widely adopted (e.g., Giroud et al. 1990, Villard et al. 2000, Lu and Miao 2015). All the points on the vertical planes are assumed to be in critical failure state. In the scope of soil arching, soil is divided into soil elements (Figure 1). The deformed soil element is depicted as a trajectory of minor principal stresses that approximates a catenary (Handy 1985). Thus, the soil arching is decided by the mobilized shear stress on the sliding surfaces. During subsidence, the deformation of soil elements gradually increases with depth (Rui et al. 2016) and depends on the deflection of geosynthetic. The deformation of the soil element, δ, can be correlated to θ as $\tan\theta = B/(4\delta)$ where θ is the angle between tangential direction of the soil element at the edge and the vertical direction, which is also the angle of major principal stress, related to the horizontal direction. For the soil elements with different deformations or stresses, the rotation of principal stress axes is considered. Thus, when the ground surface has no settlement, the overlying soil can be divided into two parts: $0 < \theta \leq \pi/4$ and $\pi/4 < \theta \leq \pi/2$. The shear stress of the soil element in the two parts can be formulated as (Feng et al. 2017a)

$$\tau_s = (\sigma_v + c\cot\varphi)\frac{4\delta B(1-K_a)}{16K_a\delta^2 + B^2} \tag{1}$$

where K_a is the coefficient of lateral earth pressure and can be defined as $K_a = \tan^2(45° - \varphi/2)$; φ and c are the internal friction angle and cohesion of the overlying soil, respectively; σ_v is the vertical stress acting on the soil element; B is the width of subsided area.

From Eq. (1), τ_s is determined by σ_v and δ of the soil element. The flat element replacing deflected soil element is analyzed based on the method proposed by Terzaghi (1943) by considering its vertical equilibrium. Then, Eq. (1) can be reformatted as

$$\frac{d\sigma_v}{dz} + \frac{8(1-K_a)\delta}{16K_a\delta^2 + B^2}(\sigma_v + c\cot\varphi) = \gamma_s \tag{2}$$

where γ_s is the unit weight of overlying soil; z is the distance between the soil element and the ground surface. Additionally, the settlement of the flat soil element is assumed to be the same as its deformation and can be formulated as

$$d\delta = \frac{\gamma_s z + q_0 - \sigma_v}{E_u}dz \tag{3}$$

where E_u is the compression modulus of the overlying soil; q_0 is the surcharge applied on the ground surface. Thus, the arching effect of overlying soil can be evaluated by combining Eqs. (2) and (3).

2.2 *Membrane effect from deflected geosynthetic*

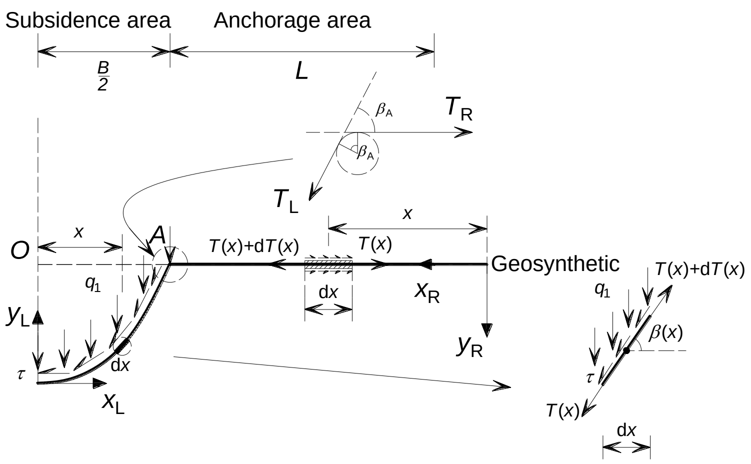

Figure 2. Equilibrium of an elementary section of geosynthetic in subsided area or anchorage area.

The deflected geosynthetic is divided into two parts: subsided area and anchorage area (Figure 1). The two areas and junction point A are analyzed separately (Figure 2). In the subsided area, the upper interface friction is considered. The interface friction between soil and geosynthetic is assumed to agree with the Coulomb friction law, and the behavior of the geosynthetic serving as a reinforcement is assumed to be linearly elastic. Based on the Coulomb friction law, there are two deformation or force types for the deflected geosynthetic in subsided area and may exist a critical sliding point (i.e., $x = x_C$ and $u = u_0$). Thus, considering force equilibrium in horizontal and vertical directions, the governing equations representing the force and deformation of deflected geosynthetic in subsided area can be formulated as

$$\begin{cases} u''(x) = 2\dfrac{q_1}{J}y'(x) + \dfrac{q_1 \tan\phi_{\mathrm{u}}}{J}\dfrac{u(x)}{u_0} & \text{if } u < u_0 \quad ① \\ u''(x) = 2\dfrac{q_1}{J}y'(x) + \dfrac{q_1 \tan\phi_{\mathrm{u}}}{J} & \text{if } u \ge u_0 \quad ② \\ y''(x) = \dfrac{q_1}{J}\dfrac{1+y'^2(x)}{u(x)} & ③ \end{cases} \tag{4}$$

where u is the tensile displacement of a s-length geosynthetic from the origin; J is the stiffness of geosynthetic; q_1 is the load over the geosynthetic in the subsided area and assumed to be uniform, which results from the overlying soil under soil arching (i.e., $q_1 = q_g$); ϕ_u is the upper interface friction angle between soil and geosynthetic.

The geosynthetic at the junction point A between the subsided and anchorage areas is assumed to form an arc shape with infinitesimal radius (Figure 2). And the vertical deformation of supporting soil in the anchorage area is also neglected. Thus, based on the analytical model proposed by Villard and Briançon (2008), the relationship between the force and deformation of stretched geosynthetic in the anchorage area can be formulated as

$$\begin{cases} u_{\mathrm{AR}} = \dfrac{T_{\mathrm{R}}}{Jm},\ K = \dfrac{u_{\mathrm{AR}}}{u_0} & \text{if } u_{\mathrm{AR}} < u_0 \quad ① \\ u_{\mathrm{AR}} = u_0 + \dfrac{T_{\mathrm{R}}^2 - T_{\mathrm{C}}^2}{2u_0 (Jm)^2},\ K = 1,\ T_{\mathrm{C}} = u_0 Jm & \text{if } u_{\mathrm{AR}} \ge u_0 \quad ② \\ m^2 = \dfrac{q_2(\tan\varphi_{\mathrm{u}} + \tan\varphi_1)}{Ju_0},\ T_{\mathrm{L}} = T_{\mathrm{R}} e^{K\beta_{\mathrm{A}}\tan\varphi_1} & ③ \end{cases} \tag{5}$$

where T_L, T_R, and T_C are the tensile forces at the left and right sides of point A and critical sliding point in the anchorage area, respectively; u_{AR} is the displacement on the right of point A. Thus, the membrane effect of deflected geosynthetic can be evaluated by combining Eqs. (4) and (5). Additionally, the supporting soil in subsided area stops the geosynthetic from deflecting, and its force and deformation relation is assumed to agree with one-dimensional compression model (i.e., $q_s = k\delta_g = E_0\delta_g/H_{sub}$ where q_s and δ_g are the force and deformation of subsoil, respectively; H_{sub} is the thickness of subsoil; E_0 is the equivalent stiffness of subsoil; k is the equivalent coefficient of subgrade reaction). The deformations of soil and geosynthetic, here, are equal. Based on the vertical equilibrium, the force relationship between overlying soil, geosynthetic and supporting soil can be obtained as $\sigma_{vH} = q_s + q_g$ where σ_{vH} is the vertical stress calculated by Eqs. (2) and (3). Thus, based on these obtained relationships, the forces and deformations of soil and geosynthetic can be calculated by combining Eqs. (2)-(5) and boundary conditions provided by Feng et al. (2017b).

3 RESULTS AND DISCUSSIONS

3.1 *Vertical stress and deformation of overlying soil*

Figure 3 shows the distributions of vertical stress and deformation with depth in the overlying soil for different equivalent coefficients of subgrade reaction in subsided area. The needed parameters are enclosed in Table 1 except k and J. To facilitate the analysis of mechanisms, the stiffness of geosynthetic is 400 kN/m. Only subsiding itself the overlying soil in subsided area can transfer its partial load to the anchorage area, that is, arching effect occurs. The load acting on the geosynthetic after subsidence is reduced. Thus, the difference between the vertical stress of subsided soil and the initial value prior to subsidence, can be used to reflect the arching effect. From Figure 3a, the vertical stress difference increases with depth in the overlying soil, which shows the effects of the arching effect on the soil element with different depths. This agrees with the results reported by Rui et al. (2016a, b). Obviously, the soil adjacent to the geosynthetic is the most affected, and its deformation is also maximal equal to the deflection of geosynthetic (Figure 3b). The deformation of overlying soil results from the deflection of geosynthetic or the subsidence of supporting soil, while its deformation difference results from the arching effect. One thing is consequently clear: soil arching caused by subsidence is also characterized by soil deformation difference between the top and bottom soil elements in the overlying soil, and the relationship between the two can be reflected by Eq. (3). From Figure 3, for the ground surface, there occurs subsidence but no arching effect. Thus, the development of arching effect depends on the subsided soil.

From Figure 3, for different equivalent coefficients of subgrade reaction, there exists an inverse correlation between vertical stress and settlement, instead of the difference between the two. The former is the result of the joint effect of geosynthetic and supporting soil. When there is no supporting soil (i.e., $k = 0$), the vertical load acting on the geosynthetic is minimal under maximal arching effect, and yet undertaken only by the deflected geosynthetic. When k = 400 kPa/m, the vertical load is maximal under minimal arching effect, and yet undertaken by both of the deflected geosynthetic and supporting soil. Meanwhile, the supporting soil play a dominant role, leading to less deformation of overlying soil. Therefore, for geosynthetic-reinforced structures, the supporting soil in subsided area should not be neglected and its force-deformation relationship is of importance.

Table 1. Geometry and material properties of the soil and geosynthetic

Property	Value
Geometry	
Width of subsided area, B (m)	1.4
Height of overlying soil, H (m)	7.2
Compression modulus of overlying soil, E_u (kPa)	15000
Overlying soil	
Unit weight, γ_s (kN/m^3)	20
Internal friction angle, φ (°)	30
Cohesion, c (kPa)	10
Geosynthetic	
Critical relative displacement between soil and geosynthetic, u_0 (m)	0.005
Upper interface friction angle between soil and geosynthetic, ϕ_u (°)	30
Lower interface friction angle between soil and geosynthetic, ϕ_l (°)	25
Surcharge applied on the ground surface, q_0 (kPa)	0

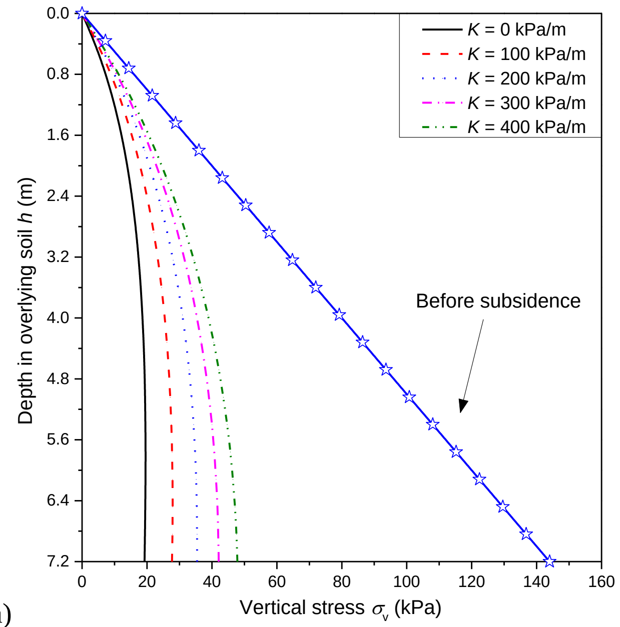

(a)

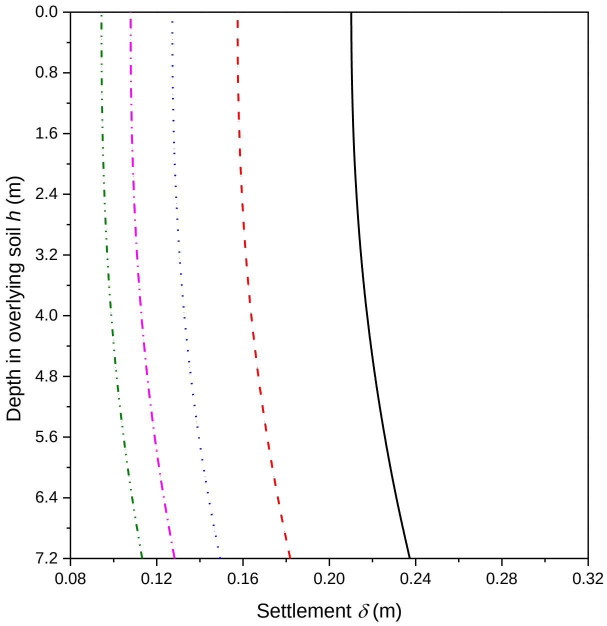

(b)

Figure 3. Distributions of vertical stress and deformation with depth in the overlying soil for different equivalent coefficients of subgrade reaction in subsided area: (a) vertical stress; (b) settlement.

3.2 *Strain and vertical displacement of geosynthetic*

Figure 4 shows the variations of strain and vertical displacement of geosynthetic for different equivalent coefficients of subgrade reaction in subsided area. After subsidence, the geosynthetic hinders the overlying soil from sinking (i.e., membrane effect), which results in the strain and vertical displacement of geosynthetic, as shown in Figure 4. Meanwhile, the membrane effect is reflected by the maximum strain and maximum vertical displacement of geosynthetic. The former occurs at the junction point A between the subsided and anchorage areas, and the latter occurs at the middle of subsided area. In Figure 4a, from the middle of subsided area to the margin of anchorage area, the strain of geosynthetic increases first in the subsided area and then decreases dramatically in the anchorage area. This agrees with the results reported by Villard and Briançon (2008). It can be seen that the stretch of geosynthetic (i.e., membrane effect), originated from subsided area, spreads towards the marginal edge of anchorage area during a subsiding process. However, the membrane effect is mainly embodied in the vicinity of point A, resulting from the anchoring effect of geosynthetic in the anchorage area. The anchoring effect depends on the load from overlying soil, the stiffness and interface friction angles of geosynthetic, and the deformation of supporting soil. Instead, the last one is not considered, which affects the results of strain and deflection. Thus, the membrane effect is decided by its surrounding soil, and its accurate estimation depends on a physical understanding of soil-geosynthetic interaction.

From Figure 4, for different k, the strain of geosynthetic has a positive correlation to its deflection. When there is no supporting soil (i.e., k = 0), both of the strain and vertical displacement of geosynthetic are maximal. With consideration of the upper interface friction in subsided area, the interaction between the overlying soil and geosynthetic increases with decreasing k. Further, based on Eq. (4), the upper interface friction promotes the developments of strain and vertical displacement of geosynthetic. Combining Figures 3 and 4, the supporting soil has great effect on both of soil arching and membrane effect. During a subsiding process, the forces and deformations of the overlying soil, geosynthetic and supporting soil occur simultaneously, and the analysis is done only based on the force equilibrium and deformation coordination between the three.

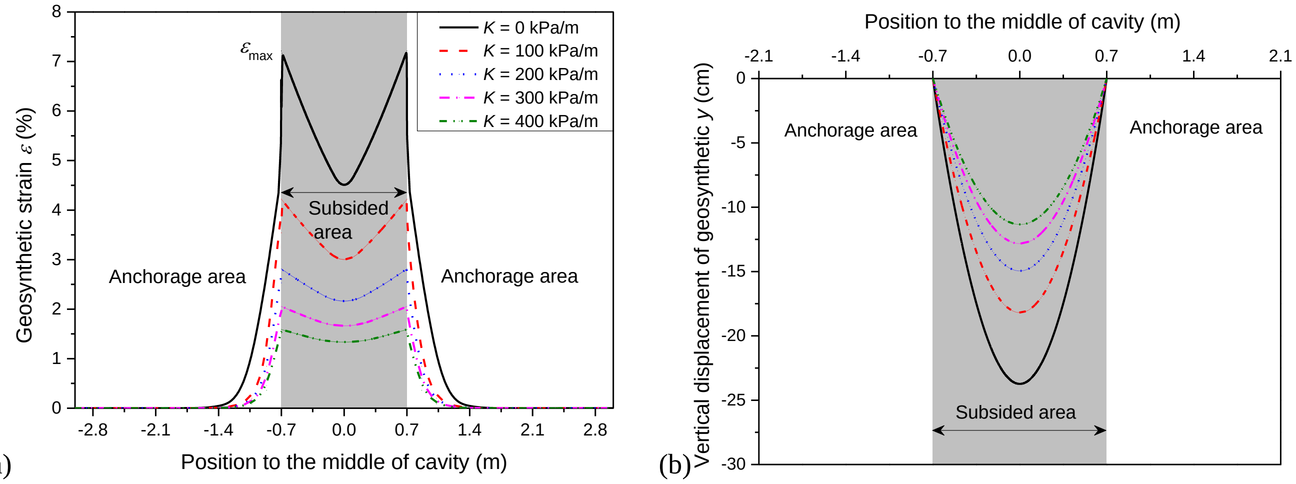

Figure 4. Strain and vertical displacement of geosynthetic for different equivalent coefficients of subgrade reaction in subsided area: (a) strain; (b) vertical displacement.

4 CONCLUSIONS

In this study, an analytical model is proposed to estimate the force and deformation characteristics in geosynthetic-reinforced structures subjected to localized sinkholes. In overlying soil, the force-deformation relationship of soil elements agrees with one-dimensional compression model. In subsided area, the upper interface friction between soil and geosynthetic is considered. Based on this, the arching effect from overlying soil is coupled with the membrane effect of deflected geosynthetic by considering the force equilibrium and deformation coordination. The coupled model is adopted to analyze the effects of supporting soil on soil arching and membrane effect. The results show that the development of arching effect depends on subsided soil, and the membrane effect is decided by its surrounding soil. Ignoring the supporting soil in subsided area leads to obvious undervaluation of arching effect and membrane effect.

REFERENCES

Briançon, L., & Villard, P. 2008. Design of geosynthetic-reinforced platforms spanning localized sinkholes. Geotextiles and Geomembranes, Vol. 26(5), pp. 416-428.

Dewoolkar, M.M., Santichaianant, K., & Ko, H.Y. 2007. Centrifuge modeling of granular soil response over active circular trapdoors. Soils and Foundations, Vol. 47(5), pp. 931-945.

Espinoza, R.D. 1994. Soil-geotextile interaction: evaluation of membrane support. Geotextiles and Geomembranes, Vol. 13(5), pp. 281-293.

Evans, C.H. 1984. An examination of arching in granular soils Master of Science Thesis in Civil Engineering. Massachusetts Institute of Technology.

Feng, S.J., Ai, S.G., & Chen, H.X. 2017a. Estimation of arching effect in geosynthetic-reinforced structures. Computers and Geotechnics, Vol. 87, pp. 188-197.

Feng, S.J., Ai, S.G., Chen, H.X., & Xie, H.J. 2017b. An analytical method for predicting load acting on geosynthetic overlying voids. Geotextiles and Geomembranes, Vol. 43(4), pp. 317-331.

Giroud, J.P., Bonaparte, R., Beech, J.F., & Gross, B.A. 1990. Design of soil layer-geosynthetic systems overlying voids. Geotextiles and Geomembranes, Vol. 9(1), pp. 11-50.

Gourc, J.P., & Villard, P. 2000. Reinforcement by membrane effect: Application to embankments on soil liable to subsidence. Proc., 2nd Asian Geosynthetics Conf.: Geosynthetics ASIA 2000, Kuala Lumpur, Malaysia, 1, Int. Geosynthetics Society, West Palm Beach, FL, pp. 55-72.

Handy, R.L. 1985. The arch in soil arching. Journal of Geotechnical Engineering, Vol. 111(3), pp. 302-318.

Lu, W., & Miao, L. 2015. A simplified 2-D evaluation method of the arching effect for geosynthetic-reinforced and pile-supported embankments. Computers and Geotechnics, Vol. 65(65), pp. 97-103.

Rui, R., Van Tol, A.F., Xia, Y.Y., Van Eekelen, S.J.M., & Hu, G. 2016a. Investigation of soil-arching development in dense sand by 2d model tests. Geotechnical Test Journal, Vol. 39(3), pp. 415-430.

Rui, R., Van Tol, A.F., Xia, X.L., Van Eekelen, S.J.M., Hu, G., & Xia, Y.Y. 2016b. Evolution of soil arching; 2D DEM simulations. Computers and Geotechnics, Vol. 73, pp. 199-209.

Terzaghi, K. 1943. Theoretical Soil Mechanics, John Wiley & Sons, New York, NY.

Van Eekelen, S.J.M., Bezuijen, A., & Van Tol, A.F. 2013. An analytical model for arching in piled embankments. Geotextiles and Geomembranes, Vol. 39, pp. 78-102.

Villard, P.V., & Briançon, L. 2008. Design of geosynthetic reinforcements for platforms subjected to localized sinkholes. Canadian Geotechnical Journal, Vol. 45(2), pp. 196-209.

Villard, P., Gourc, J.P., & Giraud, H. 2000. A geosynthetic reinforcement solution to prevent the formation of localized sinkholes. Canadian Geotechnical Journal, Vol. 37(5), pp. 987-999.

Villard, P., Huckert, A., & Briançon, L. 2016. Load transfer mechanisms in geotextile-reinforced embankments overlying voids: Numerical approach and design. Geotextiles and Geomembranes, Vol. 44(3), pp. 381-395.